Controlled Mineralisation of Carbon Dioxide: Laboratory Assessment

Risa Prameswari Putri[1]*, Sadiq J. Zarrouk[1], Mohammed Farid[1]

[1]Department of Engineering Science and Biomedical Engineering, University of Auckland, New Zealand

* Rput078@aucklanduni.ac.nz; risaprameswari@gmail.com

Keywords: *Carbon capture, CO_2, NCG reinjection, controlled mineralisation, hydroxide, calcite.*

ABSTRACT

NCG reinjection has been implemented in several geothermal power plants to reduce greenhouse gas emissions and support New Zealand's net-zero emissions targets. A major challenge for this system is that there is a potential for NCG breakthrough to the surrounding wells and leakage to the ground surface, which could result in high CO_2 gas emissions. Therefore, effective CO_2 mineralisation is essential to mitigate those risks. This study presents a series of laboratory experiments designed to evaluate suitable and cost-effective materials for CO_2 mineralisation.

Hydroxide compounds—including calcium hydroxide ($Ca(OH)_2$), potassium hydroxide (KOH), and sodium hydroxide (NaOH)—and industrial waste products were tested by injecting CO_2 into aqueous solutions of these materials. The efficiency of mineralisation was assessed via the composition and mass of solid $CaCO_3$ deposits formed. The tests were performed under varied conditions of temperature (25–60 °C), CO_2 flow rate (0.1–0.2 L/min), and reactant concentrations.

Based on the results, the most effective hydroxide mineral that has been tested for CO_2 mineralisation is Calcium Hydroxide ($Ca(OH)_2$) since it produces solid carbonate. However, due to the relatively high cost of pure $Ca(OH)_2$, other alternatives could be used for the CO_2 capturing. Waste products (e.g., burned lime and NSSC) containing 75-85% $Ca(OH)_2$ are proven to be effective in CO_2 mineralisation by precipitating $CaCO_3$ minerals from the carbonation of $Ca(OH)_2$ aqueous solutions. These waste-based sources produced significant $CaCO_3$ precipitation and present a promising low-cost alternative.

From these laboratory experiments, it is concluded that waste products containing significant $Ca(OH)_2$ can be effective for CO_2 sequestration in geothermal reinjection systems, helping to reduce the risk of NCG breakthrough by promoting near-complete mineralisation before subsurface injection.

1. INTRODUCTION

NCG reinjection back into geothermal reservoirs can improve reservoir performance by promoting boiling, increasing the enthalpy of the produced fluids, and maintaining reservoir pressure (Kaya & Zarrouk, 2017). On the other hand, there are risks of injecting NCG into the reservoir, such as potential NCG breakthrough to surrounding production wells, leakage to the surface, and porosity and permeability changes of the original rock matrix.

In New Zealand, three fields have implemented NCG reinjection, namely Te Huka (Ruiz et al., 2021), Ngāwhā (Titus et al., 2024), and Ngā Tamariki (Abd Ghafar et al., 2022). The NCG reinjection effect was evaluated on the Ngā Tamariki reservoir using the reactive transport model (Siahaan et al., 2024). The results show that there are various trends of porosity and permeability along the radial distance. Near the reinjection wellbore, there is increasing porosity and permeability due to calcite and anhydrite dissolution. On the other hand, there is a decrease in porosity and permeability in the outer region due to anhydrite precipitation. The results also show that there is increasing calcite dissolution near the wellbore with increasing NCG concentration due to the lower pH of the injection fluid.

Another study on the simulation of NCG reinjection was conducted for areas located at the Taupo Volcanic Zone, namely Wairakei, Kawerau, and Rotokawa, to determine the CO_2 and H_2S storage potential at that field (Galeczka & Chambefort, 2021). The study concludes that the mineralisation efficiency at reservoir conditions for those fields is insufficient. Maximum CO_2 mineralisation at Kawereau is only 12%, 0.7% at Rotokawa, and no CO_2 is predicted to mineralise at Wairakei. The inefficiency of CO_2 mineralisation during NCG reinjection might lead to an increase in CO_2 content in the reservoir, which can result in higher CO_2 produced at wells, contributing to increasing CO_2 emissions at the surface over time. With the current condition of NCG reinjection at New Zealand geothermal fields, further efforts are required to ensure that the CO_2 gas is efficiently mineralised before the reinjection fluids reach the production wells.

CO_2 mineralisation is one of the CO_2 trap mechanisms where the dissolved CO_2 reacts with divalent cations (e.g. Ca^{2+}, Mg^{2+}, Fe^{2+}) to form stable carbonate minerals (Kim et al., 2023). It is considered the most permanent and stable storage because the CO_2 is stored in solid forms, such as calcite ($CaCO_3$), magnesite ($MgCO_3$), or siderite ($FeCO_3$), which are thermodynamically stable and do not pose a risk of re-emission. The use of hydroxide minerals (e.g. $Ca(OH)_2$, NaOH, and KOH) may promote a faster mineralisation process. Aside from the hydroxide compounds, industrial waste products containing high hydroxide minerals are also potentially effective for use in the CO_2 capture process. It can offer a lower cost of mineralisation and reduce solid waste. Since the CO_2 is converted into solid carbonates before reinjections, the risk of leakage is greatly reduced, and post-injection monitoring programs are minimal.

This study aims to improve the effectiveness and efficiency of CO_2 capture to support the implementation of New

Zealand's NCG reinjection program and contribute to the achievement of the net-zero emission target by 2050.

2. METHODOLOGY

Laboratory experiments used for this study involve injecting CO_2 gas into solutions containing chemical products. These laboratory experiments aim to determine the mineralisation process due to CO_2 capture using several types of solutions, namely $Ca(OH)_2$, $CaCO_3$, KOH, NaOH, and industrial waste. At the end of the experiment, the deposits are weighed to determine their % recovery and analysed using XRD to identify their mineral compositions.

2.1 CO_2 Injection Testing

The solutions are put into a 1L cylinder and injected with CO_2 gas at a constant flow rate of 0.1 lpm, and the flow rate is measured using a rotameter. A pH probe is inserted into the solution to measure the pH variation throughout the injection process (Figure 1). The pH was measured using a Thermo Scientific™ Orion Star™ A211 Benchtop pH meter.

After the solution is injected with CO_2 gas, it is filtered using qualitative filter paper with various pore sizes (typically 6 to 11 µm). The filter paper, which already contains the deposited carbonate, is dried using an oven at a temperature of 40°C overnight. Then, it is weighed using an analytical balance, DENVER SI-234, to determine the final weight of the precipitate. The weight of deposits is calculated from the subtraction of the final weight from the initial weight.

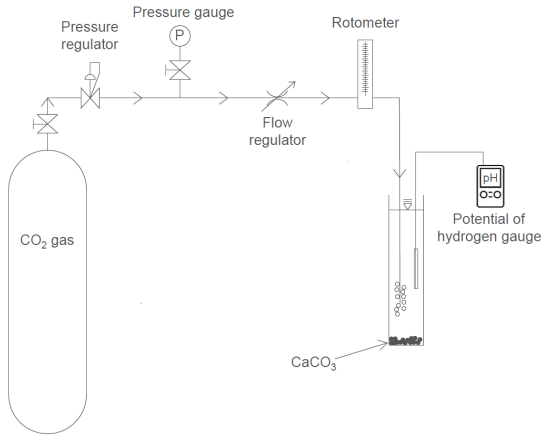

Figure 1: Schematic diagram for a CO_2-capture system using several aqueous solutions as the absorbent.

Injection of CO_2 gas into water involves several processes, including dissolution of CO_2 in water (Equation 1), formation of carbonic acid (Equation 2), and dissociation of carbonic acid (Equations 3 and 4) (Mitchell et al., 2010). These reactions (Equations 3 and 4) release H^+ ions, which lower the pH of the solution. Therefore, the injection of CO_2 into water makes the pH acidic. When the acidic pH liquid interacts with $CaCO_3$ mineral, the H^+ ions react with carbonate (CO_3^{2-}) in $CaCO_3$, shifting the equilibrium towards more dissolution (Equation 5).

$$CO_2\,(g) \rightarrow CO_2\,(aq) \quad (1)$$

$$CO_2\,(aq) + H_2O \rightleftharpoons H_2CO_3 \quad (2)$$

$$H_2CO_3 \rightleftharpoons H^+ + HCO_3^-\ (bicarbonate) \quad (3)$$

$$HCO_3^- \rightleftharpoons H^+ + CO_3^{2-}\ (carbonate) \quad (4)$$

$$CaCO_3(s) + H^+ \rightleftharpoons Ca^{2+} + HCO_3^- \quad (5)$$

Laboratory experiments are conducted to determine the effect of CO_2 injections on the $CaCO_3$ mineral, using 1 L of $CaCO_3$ solution with a CO_2 flow rate of 0.1 lpm. Three injection tests were conducted: the saturated solution (0.015 g/L water) at room temperature (National Centre for Biotechnology Information, 2025a), the supersaturated solution (10 g/L water) at room temperature, and the supersaturated solution (10 g/L water) at 80°C. After being injected with CO_2, the oversaturated solutions are filtered, dried, and weighed. The $CaCO_3$ deposit weight after CO_2 injection is shown in Table 1. Based on the results, the solution at 80°C has slightly more $CaCO_3$ loss than the solution injected at a room temperature of 22°C, although the amount is insignificant. Therefore, the experiments prove that CO_2 injection into water will dissolve $CaCO_3$ mineral due to the acidic pH solution.

Table 1: $CaCO_3$ loss calculation after CO2 injection.

Temperature (°C)	Injection Period (minutes)	Amount of $CaCO_3$ in Solution (g)	Total $CaCO_3$ after CO_2 Injection (g)	% Loss
22	30	0.015	N/A*	**N/A***
22	30	10	9.2229	**7.8%**
80	30	10	9.1434	**8.6%**

**note: in saturated $CaCO_3$ solutions (0.015 g/L water), all $CaCO_3$ are dissolved in water before the CO_2 injection and no $CaCO_3$ precipitate after CO_2 injection.*

2.2 $CaCO_3$ % Recovery Calculation

One of the injection testing experiments of CO_2 mineralisation is conducted by injecting CO_2 gas into $Ca(OH)_2$ solutions to form $CaCO_3$ minerals. The stoichiometric reaction between carbon dioxide (CO_2) and calcium hydroxide ($Ca(OH)_2$) solution to form calcium carbonate ($CaCO_3$) is as follows (Han et al., 2011):

$$Ca(OH)_2(s) + CO_2\,(g) \rightarrow CaCO_3\,(s) + H_2O\,(l) \quad (6)$$

The $CaCO_3$ % recovery refers to the amount of $CaCO_3$ formed from the injection of CO_2 gas into a $Ca(OH)_2$ solution, compared to the amount of $CaCO_3$ that should theoretically form, calculated based on stoichiometry. Therefore, the $CaCO_3$ % recovery is calculated as follows:

$$\text{CaCO3 \% recovery} = \frac{\text{weight of } CaCO_3 \text{ deposit from the experiment}}{\textit{theoretical mass of } CaCO_3} \times 100\%$$

3. HYDROXIDE CHEMICAL PRODUCTS

Several hydroxide lab-grade products are tested to determine their ability to capture and store CO_2 in the form of solid minerals. Those products include $Ca(OH)_2$, KOH, and NaOH. Solutions containing each of the products are injected with CO_2 gas under various conditions, and the deposits (if any) are weighed to determine the amount of deposits formed after CO_2 injection. The results of this experiment will be used as a basis to select which chemical is more suitable for CO_2 capture.

3.1 Injection Testing – $Ca(OH)_2$

In $Ca(OH)_2$ injection testing, the reaction conditions—such as temperature, injection period, CO_2 flow rate, and concentration—can be adjusted to determine the effect on the precipitate weight and reaction rates.

3.1.1 Temperature Effect

CO_2 injection into $Ca(OH)_2$ solutions was tested at two different temperatures, which are 22°C (room temperature) and 60°C. All solutions are in saturated conditions with respect to each temperature. At room temperature (25°C), the solubility of $Ca(OH)_2$ is 0.159 g/100 mL (Athanassiadis & Walsh, 2017). At a temperature of 60°C, the solubility is 0.116 g/100 mL (National Lime Association, n.d.). The pH trend for the tested temperatures is shown in Figure 2. It shows that $Ca(OH)_2$ solutions at the highest temperature (60°C) have a faster reaction time, which results in the faster pH decrease, possibly due to a faster reaction rate/kinetics and a smaller quantity of $Ca(OH)_2$.

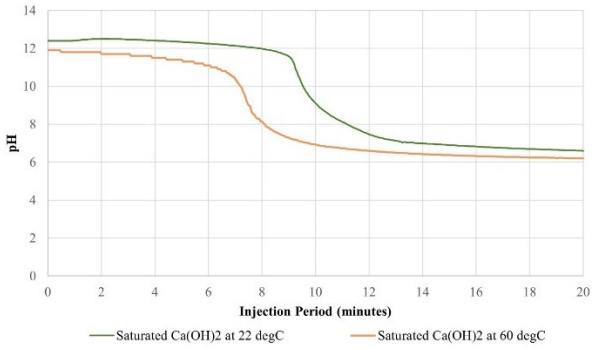

Figure 2: pH changes after CO2 injection into Ca(OH)2 solution at different temperatures.

After CO_2 injection, the solutions are filtered, and the deposits are dried to determine the weight. The amount of $Ca(OH)_2$ in solution and the % recovery at each temperature are shown in Table 2.

Table 2: Results of deposit weight and % $CaCO_3$ recovered at different temperatures.

Temperature (°C)	Amount of $Ca(OH)_2$ in Solution (g)	Total $CaCO_3$ after CO_2 Injection (g)	Calculated $CaCO_3$ (g)	% Recovery
22	1.511	1.537	2.041	**75.3%**
60	1.137	1.325	1.535	**86.3%**

The results show that the $CaCO_3$ formed at room temperature is 75.3% of the calculated $CaCO_3$, and the $CaCO_3$ formed at 60°C is 86.3% of the calculated $CaCO_3$. These higher $CaCO_3$ deposits at high temperatures may be due to the effect of $CaCO_3$ solubility. $CaCO_3$ solubility decreases with increasing temperature, which means less $CaCO_3$ can remain dissolved. Therefore, this condition leads to more precipitation of $CaCO_3$ at 60°C, compared to 22°C.

3.1.2 Injection Period Effect

Different CO_2 injection times are used to determine the effect of $CaCO_3$ formation. Two $Ca(OH)_2$ solutions at saturated conditions at room temperature are exposed to different injection periods, which are 20 minutes and 9 minutes, with a CO_2 flow rate of 0.1 lpm. In the first solution, after 20 minutes of injection, the solution pH decreased to 6.60 (Figure 3). Meanwhile, in the second solution, the pH was 9.32 after 9 minutes of injection. The deposit weight is summarised in Table 3.

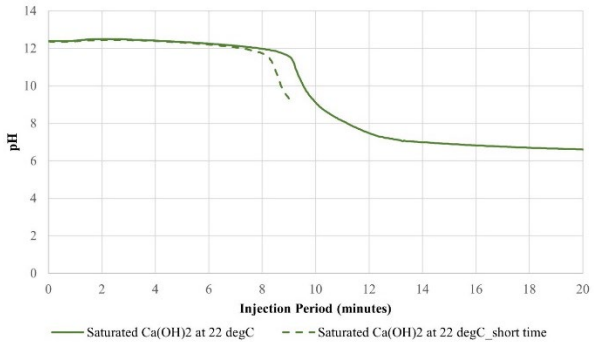

Figure 3: pH changes after CO_2 injection into $Ca(OH)_2$ solution at different injection periods.

At a shorter injection period and higher pH (pH: 9.32), the amount of $CaCO_3$ produced is more than in the longer injection period and lower final pH (pH: 6.6). This might be due to $CaCO_3$ forming effectively at a high pH range (10 < pH < initial). In the high pH range, $CaCO_3$ was produced by CO_2 absorption, which leads to a decrease in the ion concentration involved in $CaCO_3$ production, such as Ca^{2+}, CO_3^{2-}, HCO_3^-, and OH^- (Han et al., 2011). On pH range 7 to 10, there is less CO_2 absorption, increasing H^+ and HCO_3^- ion concentrations, thus, less $CaCO_3$ is formed. At a pH less than 7, CO_2 forms carbonic acid, leading to $CaCO_3$ dissolution. Therefore, a higher % recovery in a shorter injection period is because the pH is still in the high range, which is the most effective pH in $CaCO_3$ formation and no $CaCO_3$ dissolution by carbonic acid, unlike in the lower pH range.

Table 3: Results of deposit weight and % $CaCO_3$ recovered at different injection periods.

Initial pH	Final pH	Injection Period (min)	Amount of $Ca(OH)_2$ in Solution (g)	Total $CaCO_3$ after CO_2 Injection (g)	Calculated $CaCO_3$ (g)	% Recovery
12.40	6.60	20	1.511	1.537	2.041	**75.3%**
12.37	9.32	9	1.478	1.935	1.996	**96.9%**

3.1.3 CO_2 Injection Rate

As a baseline condition, the CO_2 flow rate for saturated $Ca(OH)_2$ solutions is set at 0.1 lpm at room temperature (22°C) and a higher flow rate is set using 0.2 lpm. Based on the experiment, $Ca(OH)_2$ solutions with higher CO_2 flow rates experienced a faster pH decrease because more CO_2 is dissolving per unit time, producing more H^+ ions to neutralise OH^-. Since the CO_2 flow rate is twice as high (0.2 lpm vs. 0.1 lpm), the reaction proceeds faster (half of the normal injection rate), leading to a more rapid decrease in pH (Figure 4).

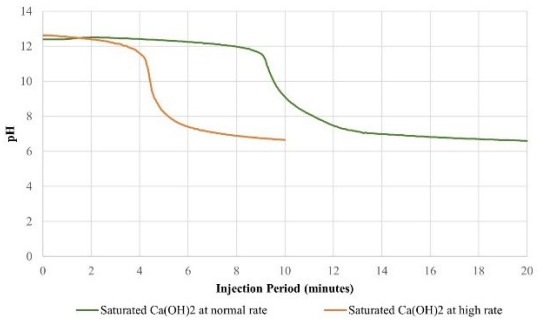

Figure 4: Saturated $Ca(OH)_2$ solutions at different CO_2 injection rates.

The results of $CaCO_3$ formation are shown in Table 4. Based on the results, the solution with a higher CO_2 flow rate has a high % recovery of $CaCO_3$, which indicates that the CO_2 can be captured effectively. A higher % recovery in higher injection CO_2 injection rates may be due to the effect of the kinetic rate increase, which introduces turbulence into the system. Turbulence produces the necessary activation energy for the precipitation process, brings more ions for the precipitation process, and enhances local supersaturation (Al-Rawajfeh, 2009). Another factor resulting in a higher % recovery in a higher injection rate is that the higher injection rate shortens the reaction time and reduces the duration of exposure to low pH conditions (shorter injection period to reach the same final pH), thereby limiting the redissolution of $CaCO_3$ into soluble bicarbonate species. Those two factors contribute to the higher % recovery at a higher injection rate.

Table 4: Results of deposit weight and % CaCO3 recovered at different CO_2 rates.

CO_2 Rates (L/min)	Sample Amount in 1L of H2O (g)	Amount of $Ca(OH)_2$ in Solution (g)	Total $CaCO_3$ after CO_2 Injection (g)	Calculated $CaCO_3$ (g)	% Recovery
0.1	1.5116	1.5109	1.537	2.041	**75.3%**
0.2	1.5007	1.2804	1.418	1.730	**82.0%**

3.1.4 Supersaturation Condition Effect

The supersaturation condition of $Ca(OH)_2$ solutions was investigated to determine its effect on the reaction rate and $CaCO_3$ recovered. Based on Figure 5, a solution with 1.5 g of $Ca(OH)_2$ dissolved in 1 L of distilled water experienced a faster pH decrease compared to the 3 g $Ca(OH)_2$ solution when injected with CO_2 at the same rate (0.1 L/min). The 1.5 g/L solution will experience a faster pH decrease because fewer OH^- ions are available to buffer against the CO_2. The 3 g $Ca(OH)_2$ solution maintains a higher pH for a longer period as a result of the buffering effects from undissolved $Ca(OH)_2$, which continuously dissolves and replenishes OH^- ions, thus resisting the acidification process for a longer period.

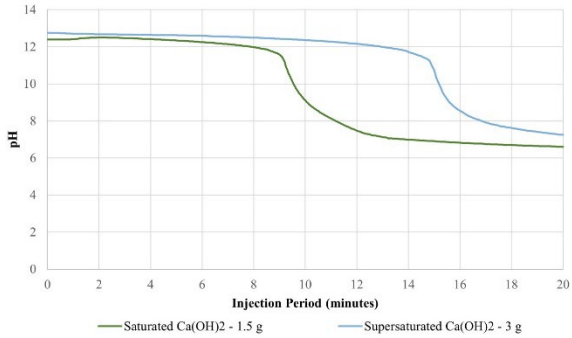

Figure 5: pH changes comparison between supersaturated $Ca(OH)_2$ solutions with saturated $Ca(OH)_2$ solutions.

The results of $CaCO_3$ formation are shown in Table 5. Based on the results, the solution with supersaturated conditions achieved a higher % recovery than the baseline conditions. These results may occur due to a higher concentration of Ca^{2+}, which shifts the carbonate equilibrium more towards the $CaCO_3$ formation. This led to increasing CO_2 absorption, more complete precipitation of $CaCO_3$, and less effect of dissolution from the carbonic acid. The experiment results confirm that a supersaturated $Ca(OH)_2$ solution could improve the precipitation efficiency in CO_2 capture systems.

Table 5: Comparison of deposit weight and % $CaCO_3$ recovered at room temperature between saturated and supersaturated conditions.

CO_2 Rates (L/min)	Amount of $Ca(OH)_2$ in Solution (g)	Total $CaCO_3$ after CO_2 Injection (g)	Calculated $CaCO_3$ (g)	% Recovery
0.1	1.5109	1.5368	2.041	**75.3%**
0.1	3.0000	3.7000	4.052	**91.3%**

3.1.5 Undersaturation Condition Effect

The undersaturated $Ca(OH)_2$ solutions were tested to determine the effect of CO_2 injection and compare it with the baseline condition/saturated solution. The undersaturated solution with 0.75 g/L was injected with a similar CO_2 rate (0.1 lpm), similar temperature (22°C), and similar injection periods (20 minutes). The pH trend changes are shown in Figure 6. The undersaturated solution experienced a faster pH decrease, almost half of the time, compared to the saturated solutions. This condition occurs because the undersaturated solution has fewer OH^- ions available to buffer against the CO_2, hence a faster pH decrease.

ISSN 2703-4275

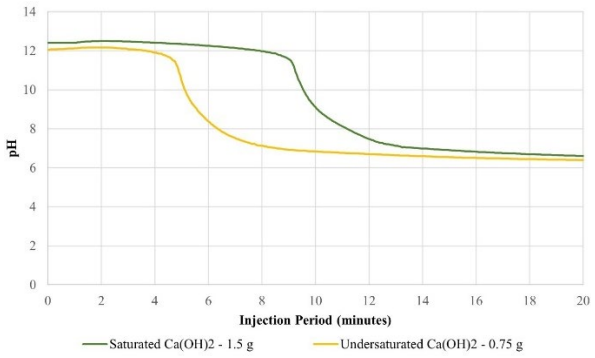

Figure 6: pH changes comparison between undersaturated $Ca(OH)_2$ solutions with saturated $Ca(OH)_2$ solutions.

The results of $CaCO_3$ deposit after 20 minutes of injections are shown in Table 6. The undersaturated solutions have less % recovery compared to the saturated solutions. This might be due to the presence of a larger amount of excess CO_2 in undersaturated solutions. If more CO_2 is added to the solutions, there will be an excess of CO_2, which promotes the formation of carbonic acid (H_2CO_3). The carbonic acid will dissolve the $CaCO_3$ deposit into soluble calcium bicarbonate ($Ca(HCO_3)_2$) and result in less $CaCO_3$.

Table 6: Comparison of deposit weight and % $CaCO_3$ recovered at room temperature between saturated and undersaturated conditions.

Solutions	Injection Period	Total $CaCO_3$ Deposit after CO_2 Injection (g)	Calculated $CaCO_3$ (g)	% Recovery
Undersaturated	20 min	0.574	1.024	**56.0%**
Saturated	20 min	1.537	2.041	**75.3%**

To prove the hypothesis of the effect of excess CO_2 on dissolving the $CaCO_3$, further experiments on saturated solutions are conducted to ensure the perfect filtration of solutions before heating up to 60°C. The results are then compared with the undersaturated solutions.

Table 7: The amount of $CaCO_3$ deposits of the undersaturated and saturated $Ca(OH)_2$ solutions.

Solutions	Amount of $CaCO_3$ deposit of solutions before heat-up (g)	Amount of $CaCO_3$ deposit of solutions after heat-up (g)	% $CaCO_3$ Produced from $Ca(HCO_3)_2$ Convertion
Undersaturated	0.2241	0.3495	60.93%
Saturated	1.0943	0.2423	18.13%
Saturated	1.072	0.2666	19.92%

Based on the weight, more calcium carbonate is produced from calcium bicarbonate (60.93%) after the heating process in the undersaturated solutions (Table 7). This proves the hypothesis that the lower % recovery in undersaturated solutions is due to more soluble calcium bicarbonate in the solution because more CO2 is present (excess CO_2).

3.1.6 Prolong Injection Rate

A longer injection period is tested at saturated $Ca(OH)_2$ solutions at room temperature to determine the dissolution effect of $CaCO_3$ by carbonic acid. The saturated solutions were injected for 3 hours at a CO_2 rate of 0.1 lpm, then it was filtered and dried to determine the deposits. The deposit weight is compared with the baseline condition (injection period: 20 minutes). The pH trend exhibits a similar time of pH decrease after CO_2 injection, which is at minute 8:50 (Figure 7).

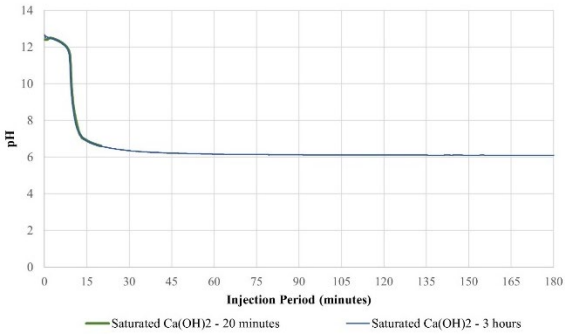

Figure 7: pH trend changes of $Ca(OH)_2$ solutions with different injection periods.

Based on the deposit weight, the solution with the longer injection period has less $CaCO_3$ amount (Table 8). It occurs because $CaCO_3$ is dissolved by carbonic acid, which results in a lower amount of $CaCO_3$ deposit after 3 hours of injection.

Table 8: Deposit weight and % recovery comparison between saturated $Ca(OH)_2$ solutions with different injection periods.

Injection Period	Amount of $Ca(OH)_2$ in Solution (g)	Total $CaCO_3$ after CO_2 Injection (g)	Calculated $CaCO_3$ (g)	% Recovery
20 minutes	1.5109	1.5368	2.041	**75.3%**
3 hours	1.5042	1.1643	2.032	**57.3%**

3.1.7 Effect of Continuous Addition of $Ca(OH)_2$

Continuous addition of $Ca(OH)_2$ into the $Ca(OH)_2$ solution (1.06 g $Ca(OH)_2$ in 1 L of distilled water) during CO_2 injection is conducted to determine its effect on the solution pH and its solubility. Figure 8 shows the pH trend during CO_2 injection and the effect on the pH after $Ca(OH)_2$ is added. After 7 minutes of CO_2 injection, the pH start to decrease and reach pH 6.72 at minutes 14:40. Then, 1 g of $Ca(OH)_2$ is added after 20 minutes of CO_2 injection, followed by 1 g after 30 minutes of injection, 1 g after 40 minutes of injection, 2 g after 50 minutes of injection, and the lastly, 2 g is added after 55 minutes of injection. The experiment was stopped after 1 hour and 20 minutes. Based on the Figure 8, there is no pH increase after $Ca(OH)_2$ was added to the solution, possibly because it did not dissolve instantaneously and deposited at the bottom of the cylinder after being added as there was no mixing involved.

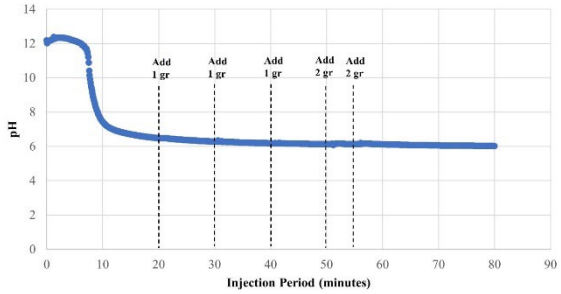

Figure 8: pH trend of continuously adding $Ca(OH)_2$ powder into the solutions during CO_2 injection.

The deposit weight and % recovery are shown in Table 9. The total deposit recovered after CO_2 injection into the solution is less than the calculated/theoretical $CaCO_3$. This might be due to the dissolution of calcite by carbonic acid, which leads to less deposit recovered at the end of the experiment.

Table 9: Calculation of $CaCO_3$ % recovery after CO_2 injection.

Temperature (°C)	Sample Amount in 1L of H_2O (g)	Total Deposit after CO_2 Injection (g)	Calculated $CaCO_3$ (g)	% Recovery
22	8.2944	9.3379	11.2043	85.70%

3.2 X-Ray Diffraction – After CO_2 Injection: $Ca(OH)_2$

XRD analysis is conducted to determine the composition of the deposit after CO_2 injection under various conditions, namely high injection rate, supersaturated, and continuous addition. Based on XRD analysis, deposits retrieved from saturated $Ca(OH)_2$ solutions that are injected by a high CO_2 flow rate (0.2 lpm) are composed of calcite ($CaCO_3$) (Figure 9).

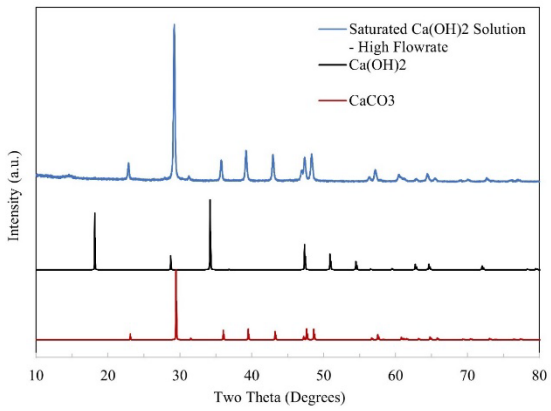

Figure 9: XRD analysis of a sample from saturated $Ca(OH)_2$ solutions injected with a high CO_2 flow rate.

Two $Ca(OH)_2$ solutions containing 3 g of $Ca(OH)_2$ in 1 L of distilled water are injected with 0.1 lpm of CO_2 for 20 minutes and 3 hours. Some samples from both conditions are analysed to determine their composition using XRD. All samples from the 20-minute and 3-hour CO_2 injection consist of $CaCO_3$ (Figure 10 and Figure 11).

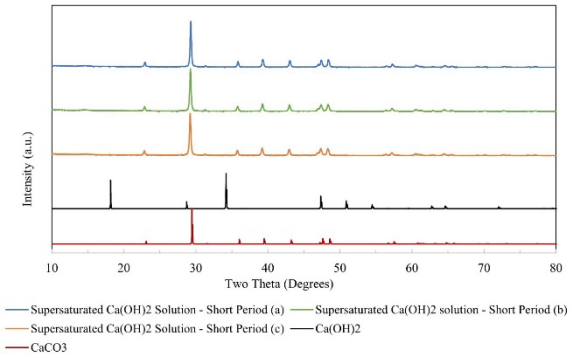

Figure 10: XRD analysis of samples from supersaturated $Ca(OH)_2$ solutions injected with CO_2 for 20 minutes.

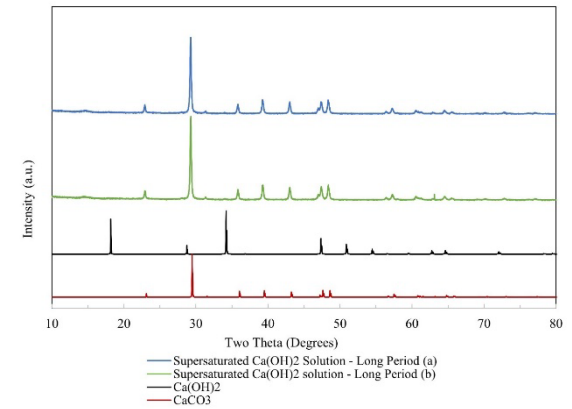

Figure 11: XRD analysis of samples from supersaturated $Ca(OH)_2$ solutions injected with CO_2 for 3 hours.

For the continuous addition of $Ca(OH)_2$, six samples from the experiment are analysed. Based on XRD analysis, three samples (samples a, e, f) contain $CaCO_3$ (Figure 12). Meanwhile, the other three samples (samples b,c,d) are composed of a mixture of $CaCO_3$ and $Ca(OH)_2$ (Figure 13).

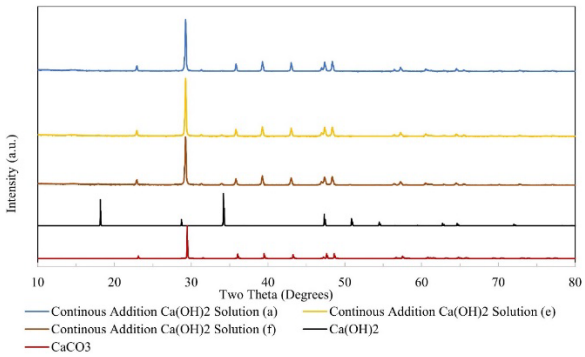

Figure 12: XRD analysis of samples a, e, and f from continuous addition of $Ca(OH)_2$ solutions injected with CO_2.

ISSN 2703-4275

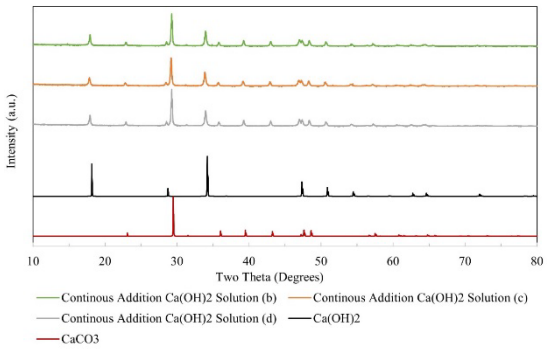

Figure 13: XRD analysis of samples b, c, and d from continuous addition of $Ca(OH)_2$ solutions injected with CO_2.

3.3 Injection Testing – Potassium Hydroxide (KOH)

KOH solution is used to determine its effect when being injected with CO_2. The primary reaction is as follows (Li et al., 2024):

$$2KOH + CO_2 \leftrightarrow K_2CO_3 + H_2O \quad (7)$$

KOH is highly soluble in water, 121 g/100 g water at 25°C (National Center for Biotechnology Information, 2025d). K_2CO_3 is also a highly soluble compound, which is 111 g/100 g water at 25°C (National Center for Biotechnology Information, 2025c). The results of pH changes after CO_2 injection into KOH solutions are shown in Figure 14. The 50 g KOH solution has a higher initial pH (13.64) because it contains more hydroxide ions (OH^-) in the solution than the 10 g KOH solution (pH: 13.18). Since the 50 g KOH solution has more OH^-, it requires more CO_2 to fully react before the pH drops. Thus, the 50 g KOH solution takes a longer time to decrease the pH.

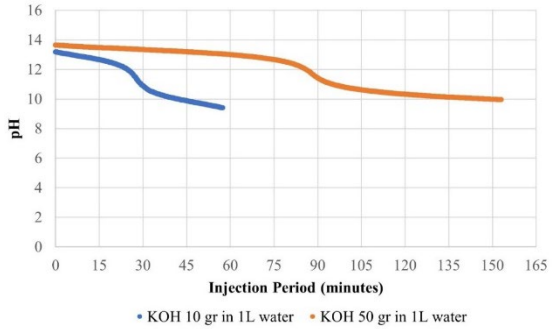

Figure 14: Results of pH changes after CO_2 injection into KOH solutions.

The experiments show that injection of CO_2 into KOH solution does not produce solid precipitated carbonate because the products (K_2CO_3 and $KHCO_3$) are highly soluble. They remain in solution and do not form stable carbonate minerals. Therefore, CO_2 is not permanently stored, but temporarily dissolved in solution.

3.4 Injection Testing – Sodium Hydroxide (NaOH)

NaOH solution is used to determine its effect when injected with CO_2. The primary reaction is as follows (Yoo et al., 2013):

$$2NaOH + CO_2 \leftrightarrow Na_2CO_3 + H_2O \quad (8)$$

NaOH is highly soluble in water, 108 g/100 g water at 25°C (National Center for Biotechnology Information, 2025e). Na_2CO_3 is also a highly soluble compound, 215 g/1L water at 25°C (National Center for Biotechnology Information, 2025b). Due to the high solubility, there is no deposition of Na_2CO_3 after CO_2 injection into an undersaturated NaOH solution. The results of pH changes after CO_2 injection into NaOH solutions are shown in Figure 15. The 50 g NaOH solution has the highest initial pH (13.26) because it contains more hydroxide ions (OH^-) in solution than the 10 g and 1.45 g NaOH solutions (pH: 13.09 and 12.5, respectively). Since the 50 g NaOH solution has more OH^- ions, it requires more CO_2 to react fully before the pH drops fully. Thus, the 50 g NaOH solution takes the longest time to decrease pH.

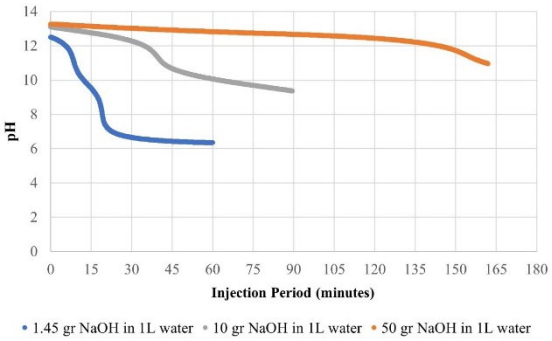

Figure 15: Results of pH changes after CO_2 injection into NaOH solutions.

Although NaOH can be used to capture CO_2, it is not suitable for permanent CO_2 storage because the products ($NaHCO_3$ and Na_2CO_3) are highly soluble, reversible, and can release CO_2 at a higher temperature. Therefore, NaOH is considered unsuitable for CO_2 mineralisation in permanent CO_2 storage in geothermal reservoirs.

Based on the experiments conducted on hydroxide solutions, $Ca(OH)_2$ is the most suitable compound for CO_2 storage via mineralisation, because it forms an insoluble solid mineral ($CaCO_3$) and is thermodynamically stable, which is essential for long-term sequestration. However, using pure $Ca(OH)_2$ can be considered high-cost. In China, the price for commercial $Ca(OH)_2$ product is USD 125/ton, and in Belgium, the price could reach up to USD 531/ton (imarc, 2024). Therefore, other alternatives for CO_2 mineralisation are using waste products that contain significant $Ca(OH)_2$ minerals.

4. WASTE PRODUCTS

Several industrial waste byproducts are tested to determine their potential and ability to absorb CO_2 gas. Waste products are used as a cost-effective alternative to $Ca(OH)_2$ powder. They are analysed using X-Ray Diffraction (XRD) to determine the mineral composition and their percentages. Samples with a significant amount of $Ca(OH)_2$ and CaO content will be used for the injection testing laboratory experiments.

4.1 Waste Products Selection

XRD patterns were collected with a PANalytical Empyrean powder X-ray diffractometer operating at 45 kV and 40 mA. A standard Cu X-ray source was employed with a Kα1 wavelength of 1.5418 Å. Materials were scanned over a two-theta range of 5 - 80° with a 0.013° step size. The phase percentages (%) are determined using the HighScore Plus

ISSN 2703-4275

Software, using known references (e.g. $CaCO_3$, $Ca(OH)_2$) to match and model the diffraction patterns. This was conducted under the supervision of an X-ray Crystallography Technologist at the School of Chemical Sciences – The University of Auckland.

The results of the waste products XRD analysis from the PANalytical Empyrean powder X-ray diffractometer and HighPlus software show that there are 2 waste products that contain significant $Ca(OH)_2$, namely burned lime (Figure 16) and NSSC (Figure 17) from the pulp and paper industry.

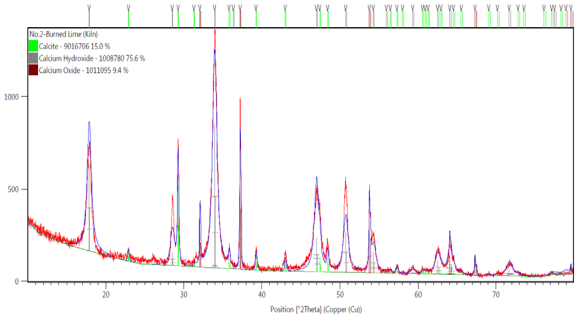

Figure 16: XRD results of the burned lime sample.

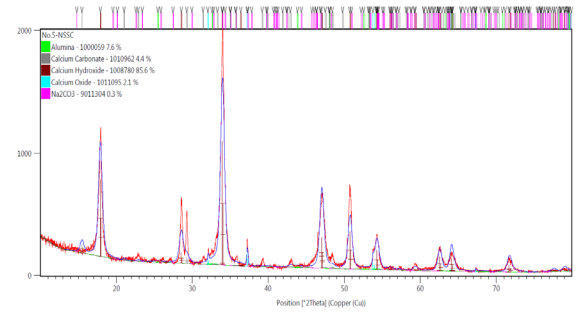

Figure 17: XRD results of the NSSC sample.

4.2 NSSC

Undersaturated and saturated NSSC solutions are tested to determine their ability to react with CO_2. The pH trend changes of undersaturated NSSC solutions are shown in Figure 18. Based on the graph, the undersaturated NSSC solutions experience an almost similar time before pH decrease compared to the undersaturated $Ca(OH)_2$ solutions, which is at ~5 minutes after CO_2 injection. Both solutions have similar pH values at the end of the experiment, which is 6.39. This indicates that at undersaturated conditions, the NSSC material with a significant $Ca(OH)_2$ content can also capture CO_2, similar to the pure $Ca(OH)_2$ powder.

The pH changes of saturated NSSC solutions and those of saturated $Ca(OH)_2$ are shown in Figure 19. The saturated NSSC solutions have a faster pH decrease (~7 minutes), compared to the saturated $Ca(OH)_2$ solutions. This might occur due to incomplete dissolution of the NSSC powder, as shown in Figure 19, where there is still a white deposit precipitated after it has been left overnight. This results in less $Ca(OH)_2$ concentration in the solution, which leads to a faster pH decrease. At the end of the experiments, both solutions have the same final pH, which is 6.6.

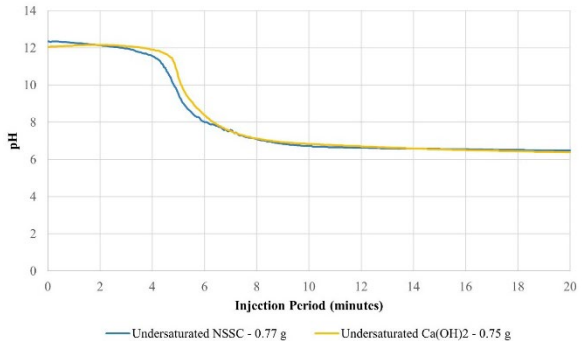

Figure 18: pH trend of undersaturated NSSC and lab-grade $Ca(OH)_2$ solution.

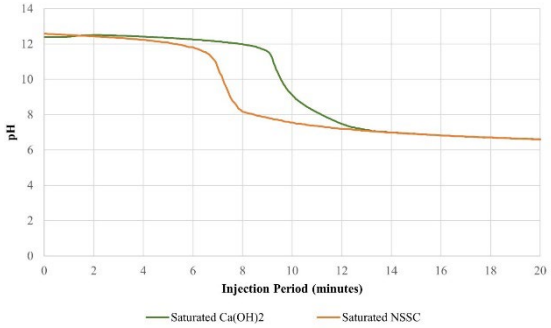

Figure 19: pH trend changes of saturated NSSC and $Ca(OH)_2$ solutions.

Based on Table 10, the undersaturated NSSC solutions have less % recovery (61.6%) compared to the saturated NSSC solutions (96.3%). The lower recovery might be due to the formation of more soluble calcium bicarbonate in the undersaturated solution due to a higher ratio of CO_2 to hydroxide, which dissolves the $CaCO_3$.

Table 10: Results of the % recovery of CaCO3 from injection testing of NSSC solutions.

Solutions	Condition	Amount of $Ca(OH)_2$ in Solution (g)	Total $CaCO_3$ Deposit after CO_2 Injection (g)	Calculated $CaCO_3$ (g)	% Recovery
NSSC	Under saturated	0.77	0.639	1.038	61.6%
NSSC	saturated	1.4	1.84	1.91	96.3%

After the CO_2 injection into the saturated and undersaturated NSSC solution, based on XRD analysis, all the deposits consist of calcium carbonate ($CaCO_3$) (Figure 20). Therefore, the NSSC solutions (both saturated and undersaturated) successfully capture CO_2 by converting the $Ca(OH)_2$ mineral into $CaCO_3$.

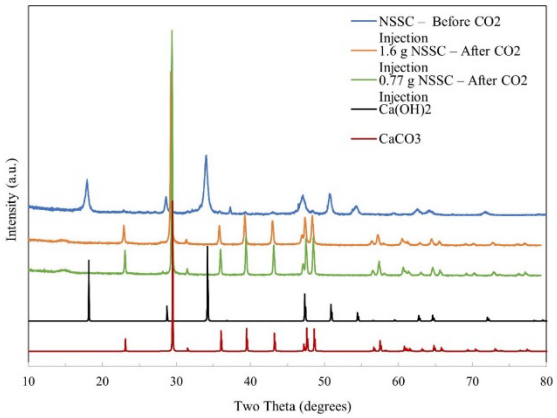

Figure 20: Results of XRD analysis of the deposit before and after CO_2 injection into the NSSC solution.

4.3 Burned Lime

Undersaturated and saturated burned lime solutions are tested to determine their effectiveness in capturing CO_2. The pH trend after CO_2 injection into the underaturated burned lime solutions is shown in Figure 21. The undersaturated burned lime solutions have a slightly faster pH decrease compared to the undersaturated $Ca(OH)_2$ solutions. This might be due to less $Ca(OH)_2$ concentration in the burned lime solutions (0.55 g of $Ca(OH)_2$ in burned lime solution vs. 0.75 g of $Ca(OH)_2$ in the $Ca(OH)_2$ solution). Both solutions have similar pH values at the end of the experiment, which is 6.39. This experiment indicates that at undersaturated conditions, the burned lime solutions containing significant $Ca(OH)_2$ can still capture CO_2, similar to the lab-grade $Ca(OH)_2$ powder.

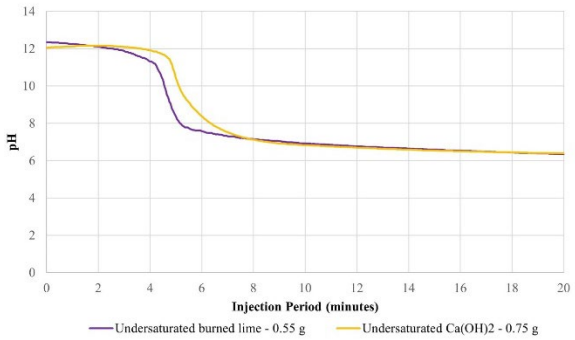

Figure 21: pH trend of undersaturated burned lime and $Ca(OH)_2$ solution.

Figure 22 shows the pH trend changes of saturated burned lime solutions and $Ca(OH)_2$ solutions. The saturated burned lime solutions experience a faster pH decrease (~6 minutes) compared to the $Ca(OH)_2$ solutions (~9 minutes). The faster decrease in pH at saturated burned lime solutions might be due to a lower $Ca(OH)_2$ concentration in the water caused by the low dissolution rate of burned lime. From the ratio of reaction time (6.4 minutes for burned lime solutions and 9 minutes for $Ca(OH)_2$ solutions), it is estimated that only 1.067 g of $Ca(OH)_2$ dissolved in the burned lime solutions instead of 1.58 g. Meanwhile, the saturated $Ca(OH)_2$ solutions have complete dissolution; thus, they have a higher $Ca(OH)_2$ concentration. A higher $Ca(OH)_2$ concentration leads to a longer reaction time before pH decreases.

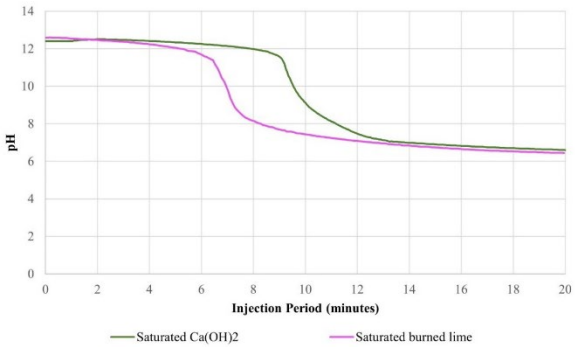

Figure 22: pH trend changes of saturated burned lime and $Ca(OH)_2$ solutions.

Based on Table 11, the undersaturated NSSC solutions have a lower % recovery (69.9%) compared to the saturated NSSC solutions (90.7%). The lower recovery might be due to more soluble calcium bicarbonate in the undersaturated solution as a result of more CO_2 excess, which dissolves the $CaCO_3$.

Table 11: Results of the % recovery of $CaCO_3$ from injection testing of burned lime solutions.

Solutions	Condition	Amount of $Ca(OH)_2$ in Solution (g)	Total $CaCO_3$ Deposit after CO_2 Injection (g)	Calculated $CaCO_3$ (g)	% Recovery
Burned lime	Under saturated	0.55	0.5239	0.749	69.9%
Burned lime	saturated	1.4	1.94	2.14	90.7%

After the CO_2 injection into the saturated and undersaturated burned lime solution, based on XRD analysis, all the deposits consist of calcium carbonate ($CaCO_3$) (Figure 23). Therefore, the burned lime solutions successfully capture CO_2 by converting the $Ca(OH)_2$ mineral into $CaCO_3$.

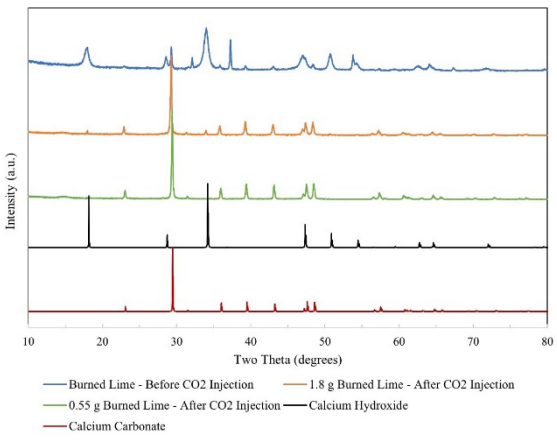

Figure 23: Results of XRD analysis of the deposit before and after CO_2 injection into the Burned Lime solution.

The experiments using waste products (namely NSSC and burned lime), which have a significant $Ca(OH)_2$ content (85% and 75%, respectively), are successfully promoting CO_2 mineralisation by precipitating it into $CaCO_3$. These products are proven to be a substitute for pure $Ca(OH)_2$ minerals at a lower cost.

5. CONCLUSIONS AND FUTURE WORKS

To support New Zealand's net-zero emissions target, this research project has proven the effectiveness of using chemical reagents and industrial waste material in optimising CO_2 mineralisation for the geothermal reinjection system. Based on the laboratory experiments that have been conducted, the following conclusions are drawn:

- Among the hydroxide compounds tested ($Ca(OH)_2$, KOH, NaOH), $Ca(OH)_2$ is the most effective for CO_2 mineralisation, because it forms a stable and solid $CaCO_3$ mineral, which is suitable for long-term storage.
- KOH and NaOH produce highly soluble carbonate products, making them unsuitable for permanent CO_2 sequestration.
- Higher temperatures (60 °C) and higher CO_2 injection rates (0.2 L/min) enhance $CaCO_3$ recovery due to faster reaction kinetics, which makes it the most effective conditions in CO2 mineralisation using Ca(OH)2 chemical reagent.
- Supersaturated $Ca(OH)_2$ solutions improve mineralisation efficiency (up to 91% recovery) by promoting complete precipitation and minimising re-dissolution by carbonic acid.
- Undersaturated conditions result in lower recovery, possibly due to the formation of more soluble calcium bicarbonate as a result of excess CO2 presence, which dissolves the CaCO3.
- With the high cost of pure $Ca(OH)_2$, industrial waste products (NSSC and burned lime) containing 75–85% $Ca(OH)_2$ were tested and achieved high CaCO3 % recovery rates (90–96%) under saturated conditions.

For future works, it is recommended to assess the possibilities of other waste products, and hydroxide compounds for cost-effective and permanent CO_2 storage. These findings support the development of low-cost, efficient CO_2 mineralisation strategies for geothermal reinjection systems and contribute to New Zealand's 2050 net-zero emissions goals**.**

ACKNOWLEDGEMENTS

This work was possible through the New Zealand Ministry of Business, Innovation and Employment (MBIE) through the Reversing Carbon Emissions in Geothermal Energy Industry – Template for Emissions – Intensive Industries project funds (UOAX2211). The author would also like to thank The University of Auckland Shared Research Equipment Platform (ShaRE) and Dr Timothy Christopher for collecting powder X-ray diffraction data.

REFERENCES

Abd Ghafar, S., Allan, G., Ferguson, A., Siega, F., Rivera, M., & Murphy, B. (2022, November 23). Non Condensable gas reinjection trial at Ngatamariki Geothermal Power Plant. *Proceedings 44th New Zealand Geothermal Workshop*.

Al-Rawajfeh, A. E. (2009). Factors influencing CaCO3 scale precipitation and CO2-H2O system in flowing water in natural water piping system. *Desalination and Water Treatment*, *12*(1–3), 337–343. https://doi.org/10.5004/dwt.2009.969

Athanassiadis, B., & Walsh, L. J. (2017). Aspects of solvent chemistry for calcium hydroxide medicaments. In *Materials* (Vol. 10, Issue 10). MDPI AG. https://doi.org/10.3390/ma10101219

Galeczka, I., & Chambefort, I. (2021, November). The potential of geothermal emissions storage in the Taupo Volcanic Zone, New Zealand. *Proceedings 43rd New Zealand Geothermal Workshop*.

Han, S. J., Yoo, M., Kim, D. W., & Wee, J. H. (2011). Carbon dioxide capture using calcium hydroxide aqueous solution as the absorbent. *Energy and Fuels*, *25*(8), 3825–3834. https://doi.org/10.1021/ef200415p

imarc. (2024). *Calcium Hydroxide pricing report 2024: price trend, chart, market analysis, news, demand, historical and forecast data*. https://www.imarcgroup.com/calcium-hydroxide-pricing-report

Kaya, E., & Zarrouk, S. J. (2017). Reinjection of greenhouse gases into geothermal reservoirs. *International Journal of Greenhouse Gas Control*, *67*, 111–129. https://doi.org/10.1016/j.ijggc.2017.10.015

Kim, K., Kim, D., Na, Y., Song, Y., & Wang, J. (2023). A review of carbon smineralisation mechanism during geological CO2 storage. *Heliyon*, *9*(12), e23135. https://doi.org/https://doi.org/10.1016/j.heliyon.2023.e23135

Li, L., Yu, H., Ji, L., Zhou, S., Dao, V., Feron, P., & Benhelal, E. (2024). Integrated CO2 capture and smineralisation approach based on KOH and cement-based wastes. *Journal of Environmental Chemical Engineering*, *12*(5). https://doi.org/10.1016/j.jece.2024.113382

Mitchell, M. J., Jensen, O. E., Cliffe, K. A., & Maroto-Valer, M. M. (2010). A model of carbon dioxide dissolution and mineral carbonation kinetics. *Proceedings of the Royal Society A: Mathematical, Physical and Engineering Sciences*, *466*(2117), 1265–1290. https://doi.org/10.1098/rspa.2009.0349

National Center for Biotechnology Information. (2025a). *PubChem Annotation Record for , CALCIUM CARBONATE, Source: Hazardous Substances Data Bank (HSDB)*. https://pubchem.ncbi.nlm.nih.gov

National Center for Biotechnology Information. (2025b). *PubChem Compound Summary for CID 10340, Sodium Carbonate*. https://pubchem.ncbi.nlm.nih.gov/compound/Sodium-Carbonate

National Center for Biotechnology Information. (2025c). *PubChem Compound Summary for CID 11430, Potassium Carbonate*. https://pubchem.ncbi.nlm.nih.gov/compound/Potassium-Carbonate

National Center for Biotechnology Information. (2025d). *PubChem Compound Summary for CID 14797, Potassium Hydroxide*. https://pubchem.ncbi.nlm.nih.gov/compound/Potassium-Hydroxide

National Center for Biotechnology Information. (2025e). *PubChem Compound Summary for CID 14798, Sodium Hydroxide*. https://pubchem.ncbi.nlm.nih.gov/compound/Sodium-Hydroxide

National Lime Association. (n.d.). *Properties of Typical Commercial Lime Products*. Retrieved March 29, 2025, from https://www.lime.org/documents/lime_basics/lime-physical-chemical.pdf

Ruiz, N. C., Kaya, E., Mclean, K., Richardson, I., Misa, T., Ferguson, A., & Altar, D. E. (2021, November 23). Passive NCG reinjection at Te Huka geothermal binary power plant. *Proceedings 43rd New Zealand Geothermal Workshop*. https://www.researchgate.net/publication/385091979

Siahaan, Y., Kaya, E., Altar, D. E., Mering, J., Subekti, D., Utami, A., Atayde, R., Melia, K., & Sepulveda, F. (2024). The 10 th Indonesia International Geothermal Convention & Exhibition (IIGCE). In *PROCEEDINGS*.

Titus, K., Dempsey, D., Peer, R., & Hanik, F. (2024). From carbon neutral to carbon negative: a theoretical bioenergy and CO2 removal retrofit at Ngāwhā geothermal power station. *Journal of the Royal Society of New Zealand*. https://doi.org/10.1080/03036758.2024.2385807

Yoo, M., Han, S.-J., & Wee, J.-H. (2013). Carbon dioxide capture capacity of sodium hydroxide aqueous solution. *Journal of Environmental Management*, *114*, 512–519. https://doi.org/https://doi.org/10.1016/j.jenvman.2012.10.061